Inner-Hydrogen Tautomerism in Some 5,15-Unsymmetrically Disubstituted and β-Unsubstituted Porphyrins

Akira TOHARA* and Mitsuo SATO

Biophysics Division, Faculty of Pharmaceutical Sciences, Teikyo University; Suwarashi, Sagamikomachi, Sagamihara, Kanagawa 229–0195, Japan. Received March 18, 2008; accepted April 10, 2008; published online April 15, 2008

5,15-Unsymmetrically disubstituted and β-unsubstituted porphyrins such as 5-R, 15-(3,5-dimethoxyphenyl) porphyrins [where R=2-benzyloxy-1-naphthyl (1), 2-(2-naphthylmethoxy)-1-naphthyl (2), anthryl (3), or 2,4,6-triphenylphenyl (4)] and 5-(2-benzyloxy-1-naphthyl), 10,15,20-tri(3,5-dimethoxyphenyl) porphyrin (1′) were synthesized and studied by ^{1}H-NMR spectroscopy. At room temperature, 1, 2, 3 and 4 showed doubling of the inner-hydrogen resonances with equal intensities, whereas the pyrrolic βH signals were completely averaged. For 1 and 1′, variable-temperature ^{1}H-NMR experiments were also performed. For 1, the two peaks of the inner hydrogen coalesced at about 313 K. In contrast, the pyrrolic βH signals were only slightly broadened even at 213 K. On the other hand, 1′ showed ordinary singlets of the inner hydrogens at room temperature, and the resonances of both the inner hydrogens and the pyrrolic βH coalesced at about 233 K. We interpret these results as indicating the existence of two distinct paths, one slow and the other fast, leading to NH tautomerization in 1. We discuss the structures and energies of *cis*-tautomers as transition intermediates in relation to the two paths of NH tautomerization.

Key words porphyrin; inner-hydrogen tautomerism; variable-temperature ^{1}H-NMR; 5,15-disubstituted and β-unsubstituted porphyrin; 5,15-disubstituted porphyrin

Porphyrins are finding uses in medicine for the treatment of cancer and dermatological diseases and in materials science as components of electronic devices.[1,2] The two hydrogen atoms in the inner part of the skeleton of a porphyrin free base are known to migrate in a framework of four nitrogen sites. This process of double hydrogen atom transfer in a porphyrin free base is also known as NH tautomerization.[3] An understanding of the mechanism of the inner-hydrogen tautomerization process is mandatory for potential technological application of porphyrins. For this reason, tautomeric exchange of the inner hydrogens of a porphyrin free base has been the subject of numerous theoretical[4—9] and experimental[10—19] studies. Most of the theoretical studies have attempted to establish a comprehensive mechanistic and kinetic basis for NH tautomerization by means of various molecular orbital calculations. Experimental studies often use dynamic NMR methods because the frequency of inner-hydrogen migration is fitted to NMR spectroscopy.

It is now generally accepted both theoretically and experimentally that (i) the two *trans*-isomers are the most stable of the isomers, (ii) any porphyrin free base is subject to tautomerism between *trans*-isomers I and II, and (iii) in NH tautomerization, the double proton transfer occurs *via* a two-step mechanism involving a metastable *cis*-intermediate rather than by a synchronous one-step path (Chart 1).

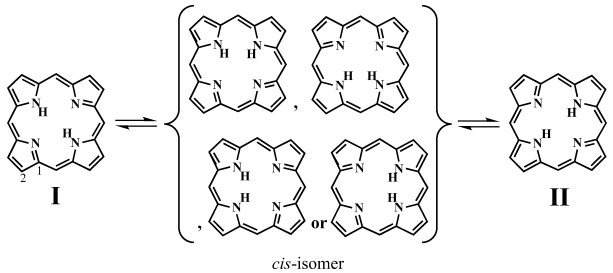

Chart 1. NH Tautomerization between 2 *trans*-Isomers I, II *via cis*-Isomer as a Transient Intermediate

In order to probe NH tautomerization by dynamic ^{1}H-NMR spectroscopy, the magnetic environment of the targeted protons must vary during the tautomerization between I and II. Pyrrolic β-hydrogens satisfy this condition in any porphyrin because their magnetic environment definitely changes during the tautomerization. However, the inner hydrogens can act as probes only when the compound has particular asymmetry, such as 5,15-unsymmetrically disubstituted porphyrins.

It should be noted that two paths (the k_1 and k_2 processes) exist for the NH tautomerization between the *trans*-isomers I and II (Chart 2). Variable temperature NMR signals of the inner protons in 5,15-unsymmetrically disubstituted porphyrins reflect only the k_1 process and thus measure a value of $2k_1$. On the other hand, the βHs probe the sum of the k_1 and k_2 processes and their signals measure a value of $2(k_1+k_2)$. Therefore, observation of the spectral behaviors of both the NHs and the βHs by variable temperature NMR spectroscopy can provide details of both the k_1 and k_2 processes. To our knowledge, however, studies of multiple

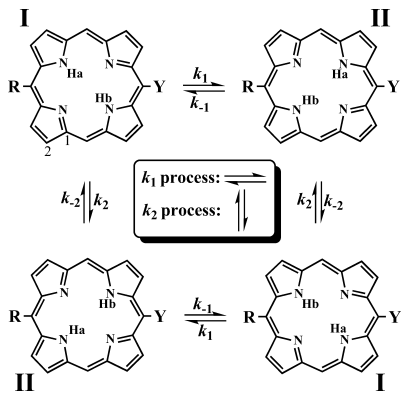

Chart 2. NH Tautomerization between 4 *trans*-Isomers

k_1 and k_2, the name of each process, are also used for the corresponding rate constant as illustrated.

* To whom correspondence should be addressed. e-mail: toharakr@pharm.teikyo-u.ac.jp

processes simultaneously in one system have been limited.[17—19)]

Ogoshi and coworkers reported anomalously slow NH tautomerization in *meso*-monosubstituted OEP, which showed doubling of the inner hydrogens in their room temperature NMR spectra.[10)]

Their work prompted us to investigate the inner-hydrogen migration in 5,15-unsymmetrically disubstituted and β-unsubstituted porphyrins especially for verifying the existence of two distinct paths for NH tautomerization. Here we report the syntheses of 5-(2-benzyloxy-1-naphthyl),15-(3,5-dimethoxyphenyl)porphyrin **1** and its related compounds **2**, **3**, **4** and **1′** (Fig. 1) and variable-temperature ^{1}H-NMR spectra of **1** and **1′**, revealing evidence for two distinct paths of NH tautomerization. The difference between the rates of the two paths is discussed in relation to the structures and energies of intermediate *cis*-tautomers.

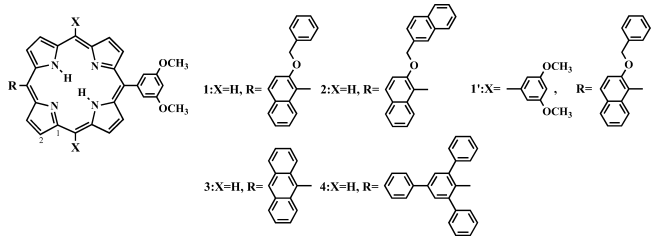

Fig. 1. 5,15-Unsymmetrically Disubstituted and β Unsubstituted Porphyrins Studied in This Work

Results and Discussion

NH and βH Resonances for 1, 2, 3 and 4 at Room Temperature The ^{1}H-NMR spectra at room temperature for **1**, **2**, **3** and **4** in $CDCl_3$ are shown in Fig. 2. They reveal two distinct singlets of equal intensity for the NH groups at room temperature ($\delta = -2.94$ and -3.02 for **1**, -2.91 and -2.99 for **2**, -2.84 and -2.96 for **3** and -3.25 and -3.36 for **4**). The frequency differences in the signals were estimated to be 53 Hz for **1**, 48 Hz for **2**, 75 Hz for **3** and 69 Hz for **4**. Two in-

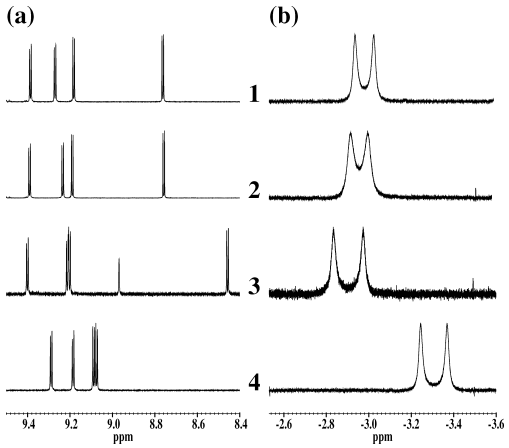

Fig. 2. ^{1}H-NMR Spectra at Room Temperature for **1**, **2**, **3** and **4**

(a) β pyrrolic H region and (b) pyrrolic NH region. Peak at 9.0 ppm of **3** is assigned to anthryl proton.

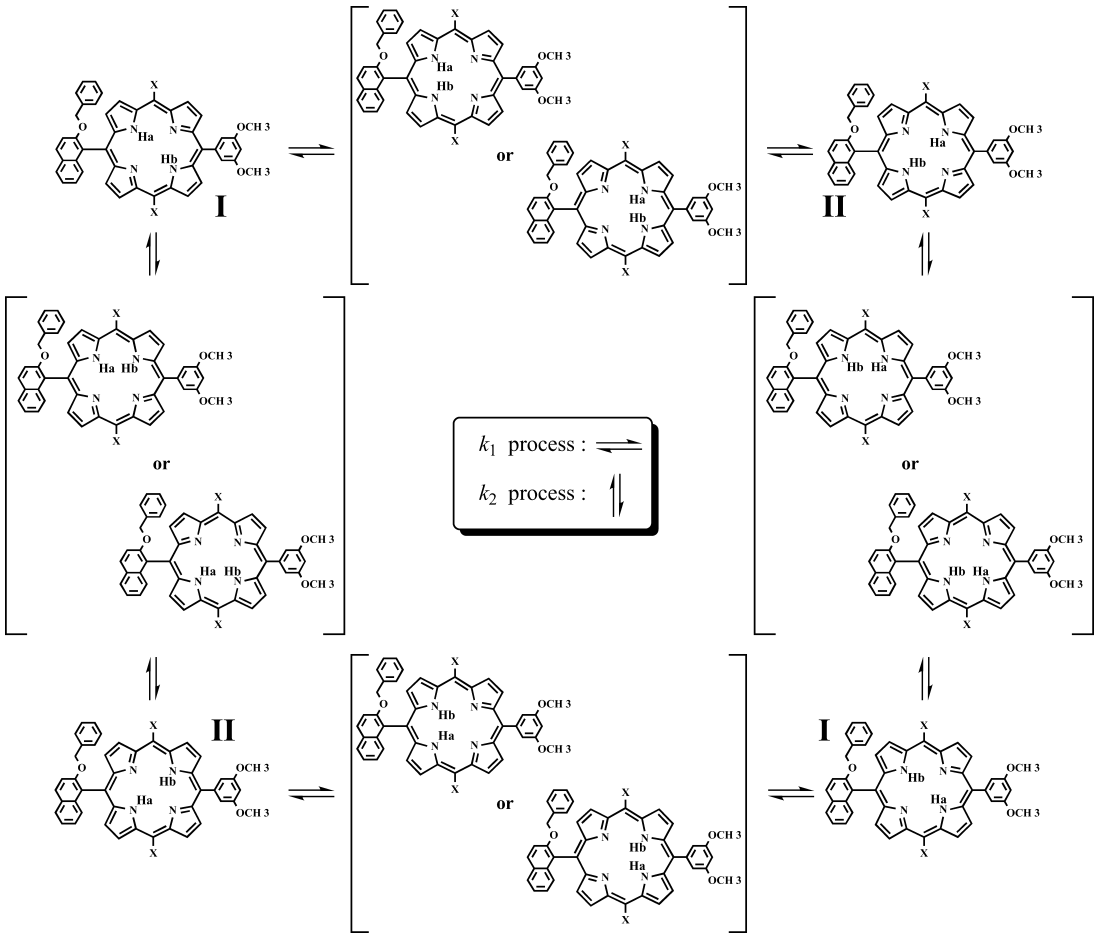

Chart 3. NH Tautomerizations between *trans*-Isomers I and II *via cis*-Isomers in **1** (X=H) and **1′** (X=3,5-Dimethoxyphenyl)

terpretations arise from these observations: (a) the two inner protons in the *trans*-isomers exist in different magnetic environments, and (b) the rates of NH tautomerization are anomalously low (see later). (a) is apparently a result of 5,15-unsymmetrical substitution, and the ring current effect caused by 5- and 15-unsymmetrical substituents is likely to be important. For (b), it should be emphasized that this phenomenon involves only slowing of the k_1 process, as the k_2 process will never result in differences in the magnetic environments of the inner hydrogens (Chart 3).

In contrast to the resonances of the inner protons, those of βH showed ordinary sharp doublets. The two signals arising from the pyrrole rings with and without a proton on the pyrrole nitrogen coalesced completely.[20] As the spectral behaviors of βH should reflect the sum of the k_1 and k_2 processes, these observations reveal that the rate of the k_2 process is much higher than that of the k_1 process in NH tautomerization in **1**, **2**, **3** and **4**.

Variable-Temperature ^{1}H-NMR Spectroscopy for 1 and 1′ Spectra in the NH resonant region for compound **1** in the range 293 to 323 K, reflecting only the k_1 process, are shown in Fig. 3a along with the calculated spectra. The rate constants k_1 were determined, as indicated in Fig. 3b, so as to simulate the observed spectra.[21] Plots of $\ln 2k_1$ *vs.* $1/T$ according to the Arrhenius equation, $\ln 2k_1 = \ln A - E_a/RT$ (E_a; acitvation energy, $\ln A$; frequency factor), gave a straight line with E_a (kcal/mol)=9.6 and $\ln A$=20.2. The rates, activation energies E_a and frequency factor $\ln A$ are summarized for the k_1 process in Table 1. Retardation of the k_1 process in **1** at room temperature was again confirmed by the data. The spectra for compound **1** in the range 223 to 273 K are shown in Fig. 4. The frequency difference between the two peaks in the NH resonant region was estimated to be 64 Hz at 223 K. All of the βH signals were only slightly broadened, indicating that they were almost averaged even at 223 K. This observation contrasts with the coalescence temperature of *ca.* 313 K for NH resonance. These results demonstrate a marked and surprising difference between the rates of the k_1 and k_2 processes in **1**.

For comparison, variable-temperature ^{1}H-NMR spectroscopy of **1′** was also performed, and the spectral behaviors are shown in Fig. 5. The frequency difference between the two peaks for NH resonance at 213 K was estimated to be 56 Hz. The rate constants k_1 were determined so as to simulate the observed spectra. Plots of $\ln 2k_1$ *vs.* $1/T$ according to the Arrhenius equation, $\ln 2k_1 = \ln A - E_a/RT$, gave a straight line with E_a (kcal/mol)=6.6 and $\ln A$=19.2 (Table 1). The two peaks of the inner hydrogens coalesced at about 233 K. This is 80 K lower than the coalescence temperature for **1**.

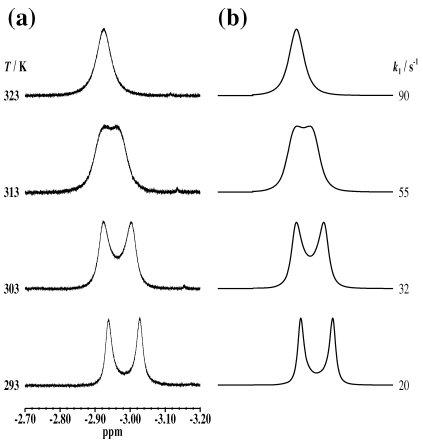

Fig. 3. Experimental (a) and Calculated (b) 600-MHz ^{1}H-NMR Spectra for the Nitrogen-Bonded Inner Protons of Compound **1** in $CDCl_3$ as a Function of Temperature

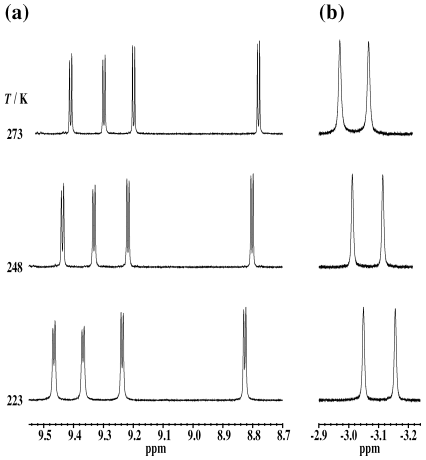

Fig. 4. ^{1}H-NMR Spectra for Compound **1** in $CDCl_3$ in the Range of 223 to 273 K

(a) βH regions and (b) NH regions.

Table 1. The Rates and Activation Parameters of k_1 Process for **1** and k_1 and k_2 Processes for **1′**

Temperature (K)	**1**			**1′**					
	k_1 process			k_1 process			k_2 process		
	$2k_1$ (s^{-1})	E_a (kcal·mol^{-1})	$\ln A$	$2k_1$ (s^{-1})	E_a (kcal·mol^{-1})	$\ln A$	$2k_2$ (s^{-1})	E_a (kcal·mol^{-1})	$\ln A$
323	180	9.6	20.2	—	—	—	—	—	—
313	110	9.6	20.2	—	—	—	—	—	—
303	65	9.6	20.2	—	—	—	—	—	—
293	39	9.6	20.2	2700[a]	—	—	—	—	—
253	—	—	—	446	6.6	19.2	114	7.0	18.7
243	—	—	—	260	6.6	19.2	62	7.0	18.7
233	—	—	—	136	6.6	19.2	34	7.0	18.7
223	—	—	—	78	6.6	19.2	18	7.0	18.7
213	—	—	—	38	6.6	19.2	8	7.0	18.7

a) Extraporated value.

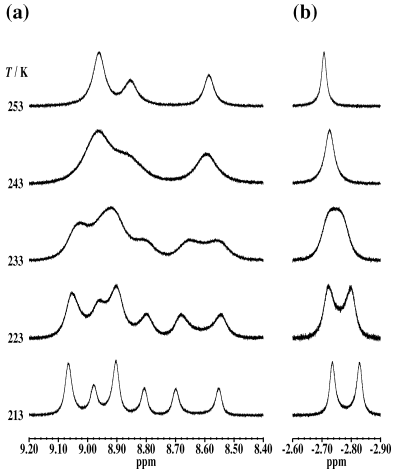

Fig. 5. ^{1}H-NMR Spectra for Compound **1′** in $CDCl_3$ in the Range of 213 to 253 K

(a) βH regions and (b) NH regions.

The difference between the rates of process k_1 in **1** and **1′** is caused by the difference in activation energy E_a (6.6 kcal/mol for **1′** and 9.6 kcal/mol for **1**) rather than in frequency factor $\ln A$ (19.2 for **1′** and 20.2 for **1**).

On the other hand, by simulation of βH signals (for simplicity, signals of H3 and H7 at 8.50—8.75 ppm were used) as a function of temperature, the values of $2(k_1+k_2)$ were determined as 46, 90, 164, 322 and 560 s^{-1} for T=213, 223, 233, 243 and 253 K respectively. The values of $2k_2$ then were calculated by subtracting $2k_1$ from $2(k_1+k_2)$ (Table 1). Plots of $\ln 2k_2$ *vs.* $1/T$ according to the Arrhenius equation, $\ln 2k_2 = \ln A - E_a/RT$, gave a straight line with E_a (kcal/mol)=7.0 and $\ln A$=18.7 (Table 1).

The difference between the rates of the k_1 and k_2 processes, therefore, seems to be small in **1′**, in contrast to **1**. Consequently, the observations suggest that compound **1** differs from compound **1′** in the mechanisms determining the rates of NH tautomerization.

Preliminary Explanation for Relations between the Rates of NH Tautomerism and Structures of *cis* Isomers as Intermediates The results for NH tautomerism, when moving from compound **1′** which is fully substituted at the *meso* positions to compound **1** which is substituted at the 5- and 15-positions, show that the rate of the k_1 process decreases and the rate of the k_2 process increases. Therefore, the specific difference between the rates of the k_1 and k_2 processes in **1** must be due to the effects of these structural perturbations imposed by *meso*-substituents on the activation energies for NH tautomerism.

The crystal structure of free base 5,10,15,20-tetraphenylporphyrin, the prototypical one of *meso* fully substituted porphyrin, is basically square, with distances between adjacent N atoms of 2.91±0.01 Å and C_α–C_{meso}–C_α angles of 125.4±0.1 degrees.[22] In contrast, free base 5,15-diphenylporphyrin (DiPP), the prototypical one of 5,15-disubstituted porphyrin, is elongated along the 5,15 axis with N–N distances of 3.06 Å (along the 5–15 axis) and 2.76 Å (along the 10–20 axis).[23] The C_α–C_{meso}–C_α angles are contracted at the 5,15 positions (122.7±0.1 degrees) and expanded at the 10,20 positions (129.0±0.2 degrees). This elongation is clearly a result of the phenyl substituents.

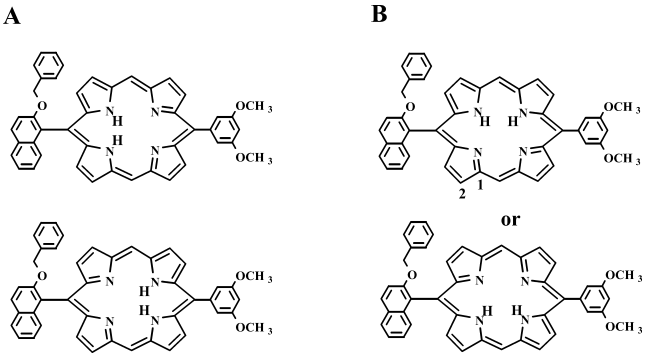

Chart 4. Structures of *cis*-Isomers as Transient States in k_1 (A) and k_2 (B) Process in NH Tautomerism

The deformation of porphine core is exaggerated for clarity.

It seems natural to consider that **1** is elongated along the 5–15 axis as DiPP whereas **1′** is approximately square. It is then possible to qualitatively predict the effect of elongating the core in **1** on the energies of the intermediate *cis* states. Compared to **1′**, elongation along the 5–15 axis in **1** has to increase the energy of the *cis* tautomer for process k_1 (due to greater steric crowding of the inner hydrogen atoms). Conversely, the *cis* tautomer for process k_2 is less sterically crowded because of the larger N–N distance (Chart 4).

Although these interpretations may be simplistic, they seem to account for substantial features of the characteristic rates of inner-proton migration in **1**, **1′**, **2**, **3** and **4**.[24]

Conclusion

^{1}H-NMR spectroscopy was performed for compounds **1**, **2**, **3**, **4** and **1′**, which are 5,15-nonsymmetrically disubstituted and β-unsubstituted porphyrins that are simple in structure and relatively easy to synthesize. Observations of both NH and βH suggested the existence of two distinct paths, one fast and the other slow, for NH tautomerism in **1**.

The crystal structures of TPP and DiPP in the literature have suggested the geometry of the *cis*-porphyrin isomer, and we used this information to interpret the two distinct paths for NH tautomerism in **1** in terms of steric crowding of the inner hydrogen atoms in the *cis* isomer as a transition intermediate.

Currently, we are studying in more detail the temperature dependency of the NMR spectra of **1**, **1′**, **2**, **3**, **4**, other kinds of 5,15-nonsymmetrically substituted β-unsubstituted porphyrins and *meso*-partially substituted porphyrins, and also beginning X-ray analysis of **1**, **2**, **3** and **4**.

Experimental

General Methods Chloroform used as the reaction medium was dried over 4A molecular sieves for several days and used after decantation. Dipyrromethane was prepared by a literature procedure.[25] Other chemicals were obtained from Aldrich or Tokyo Kasei and used without further purification. Chromatography was performed on FUJI SILYSIA CHEMICAL Micro Bead 4B silica gel. ^{1}H-NMR spectra (600 MHz) were recorded with $CDCl_3$ as solvent on a JEOL ECP-600 spectrometer. Chemical shifts (δ) are expressed in ppm relative to TMS.

Syntheses. Preparation of Aldehydes Details of experimental conditions used in the preparation of 2-bezyloxy-1-naphthaldehyde (**1a**) is reported here. The preparation of 2-(2-naphthylmethoxy)-1-naphthaldehyde (**2a**) was carried essentially by the detailed procedures reported for **1a**.

2-Benzyloxy-1-naphthaldehyde A 50 ml flask was charged with 30 ml of DMF. 8.6 g (0.05 mol) of 2-hydroxy-1-naphthaldehyde, 8.6 g (0.05 mol) of

benzylbromide and 13.8 g of anhydrous K_2CO_3 were added, and the solution was stirred magnetically at 80° for 30 min. The reaction mixture was filtered to remove K_2CO_3. Ether was added to the filtrate and the mixture was washed with water. The resulting solution was dried with Na_2SO_4 and evaporated. The residue was reprecipitated from dichloromethane–methanol, affording 10.49 g (80.1%) of pure aldehyde (light yellow crystals). *Anal.* Calcd for $C_{18}H_{14}O_2$: C 82.42, H 5.38%; Found: C 82.19, H 5.38%. ^{1}H-NMR: δ 5.34 (s, 2H, C$\underline{H}_2$), 7.30—7.50 (m, 7H), 7.62 (td, 1H), 7.77 (d, 1H), 8.03 (d, 1H), 9.28 (d, 1H), 10.98 (s, 1H, C$\underline{H}$O). MS (ESI+): *m/z* obsd. 263.1050, calcd. 263.1072 $[M+H]^+$.

2-(2-Naphthylmethoxy)-1-naphthaldehyde, 2a White crystal. Yield: 59.3%. *Anal.* Calcd for $C_{22}H_{16}O_2$: C 84.59; H 5.16; Found: C 84.55; H 5.06%. ^{1}H-NMR: δ 5.51 (s, 2H, C$\underline{H}_2$), 7.39 (d, 1H), 7.43 (tm, 1H), 7.49—7.54 (m, 2H), 7.56 (dd, 1H), 7.63 (tm, 1H), 7.77 (dt, 1H), 7.86 (quar, 2H), 7.90 (d, 1H), 7.91 (s, 1H), 8.03 (d, 1H), 9.30 (d-quar, 1H), 11.04 (s, 1H, C$\underline{H}$O). MS (ESI+): *m/z* obsd. 335.1057 , calcd. 335.1048 $[M+H]^+$.

Preparation of 5,15-Unsymmetrically Disubstituted and β Unsubstituted Porphyrins Details of experimental conditions used in the preparation of 5-(2-benzyloxy-1-naphthyl),15-(3,5-dimehoxyphenyl)porphyrin (**1**) is reported here. The preparation of the other porphyrins (**2**, **3**, **4**) were carried essentially by the detailed procedures reported for **1**.

5-(2-Benzyloxy-1-naphthyl),15-(3,5-dimehoxyphenyl)porphyrin, 1 Condensation of dipyrromethane (0.5 mmol),[25] 2-benzyloxy-1-naphthaldehyde (0.25 mmol) and 3,5-dimethoxybenzaldehyde (0.25 mmol) started upon addition of $BF_3 \cdot OEt_2$ (0.33 mmol) at room temperature in dry chloroform (100 ml) under Ar atmosphere. After 1 h, the yield of porphyrinogen reached a maximum value, and a stoichiometric amount of DDQ dispersed in benzene was added quickly to convert the porphyrinogen to porphyrin. After evaporation of the solution to dryness, the residue was redissolved in a minimum of CH_2Cl_2 and chromatographed over a column of silica gel with CH_2Cl_2 as eluent. The eluate from the second red-fluorescent band was collected and again chromatographed over a column of silica gel with CH_2Cl_2–hexane (3 : 1) as eluent. The elute was evaporated and the residue was reprecipitated from dichloromethane–methanol, affording 28.4 mg (33.5% based on the statistical yield) of pure **1** (purple crystal). *Anal.* Calcd for $C_{45}H_{34}N_4O_3$: C 79.63, H 5.05, N 8.25%; Found: C 79.57, H 5.04, N 8.22%. ^{1}H-NMR: δ −3.02 (s, 1H, N$\underline{H}$), −2.94 (s, 1H, N$\underline{H}$), 4.01 (d, 6H, OC$\underline{H}_3$), 5.00 (s, 2H, C$\underline{H}_2$), 6.54—6.57 (dm, 2H), 6.71 (tm, 2H), 6.83—6.87 (m, 2H), 6.94 (t, 1H), 6.98 (tm, 1H), 7.35 (tm, 1H), 7.47 (dm, 2H), 7.75 (d, 1H), 8.06 (dt, 1H), 8.28 (dd, 1H), 8.76 (d, 2H, pyrrole βH), 9.189 (d, 2H, pyrrole βH), 9.27 (d, 2H, pyrrole βH), 9.39 (d, 2H, pyrrole βH), 10.27 (s, 2H, *meso*H). MS (ESI+): *m/z* obsd. 679.2719, calcd. 679.2709 $[M+H]^+$.

5-(2-(2-Naphthylmethoxy)-1-naphthyl),15-(3,5-dimehoxyphenyl)porphyrin, 2 Purple crystal. Yield: 41.4%. *Anal.* Calcd for $C_{49}H_{36}N_4O_3$: C 80.75; H 4.98; N 7.69%. Found: C 80.82; H 4.97; N 7.70%. ^{1}H-NMR: δ −2.99 (s, 1H, N$\underline{H}$), −2.91 (s, 1H, N$\underline{H}$), 4.02 (s, 6H, OC$\underline{H}_3$), 5.13 (s, 2H, C$\underline{H}_2$), 6.57—6.62 (m, 2H), 6.75 (s, 1H), 6.93—6.97 (m, 3H), 7.00—7.03 (m, 1H), 7.09 (d, 1H), 7.16 (tm, 1H), 7.37 (tm, 1H), 7.40 (dd, 1H), 7.48 (m, 2H), 7.79 (d, 1H), 8.06 (dm, 1H), 8.28 (d, 1H), 8.76 (d, 2H, pyrrole βH), 9.19 (d, 2H, pyrrole βH), 9.23 (d, 2H, pyrrole βH), 9.39 (d, 2H, pyrrole βH), 10.26 (s, 2H, *meso*H). MS (ESI+): *m/z* obsd. 729.2867, calcd. 729.2866 $[M+H]^+$.

5-(9-Anthryl),15-(3,5-dimehoxyphenyl)porphyrin, 3 Purple crystal. Yield: 32.5%. *Anal.* Calcd for $C_{42}H_{30}N_4O_2$: C 81.01; H 4.86; N 9.00%; Found: C 80.06; H 4.66; N 9.08%. ^{1}H-NMR: δ −2.96 (s, 1H, N$\underline{H}$), −2.84 (s, 1H, N$\underline{H}$), 4.03 (s, 6H, OC$\underline{H}_3$), 6.95 (t, 1H, $H_{4''}$), 6.98—7.01 (qua-d, 2H, $H_{2'}$, $H_{7'}$), 7.04—7.07 (dd, 2H, $H_{1'}$, $H_{8'}$), 7.46—7.50 (m, 4H, $H_{2''}$, $H_{6''}$, $H_{3'}$, $H_{6'}$), 8.32 (d, 2H, $H_{4'}$, $H_{5'}$), 8.46 (d, 2H, pyrrole βH), 8.97 (s, 1H, $H_{10'}$), 9.210 (d, 2H, pyrrole βH), 9.211 (d, 2H, pyrrole βH), 9.40 (d, 2H, pyrrole βH), 10.28 (s, 2H, *meso*H). MS (ESI+): *m/z* obsd. 623.2426, calcd. 623.2447 $[M+H]^+$.

5-(2,4,6-Triphenylphenyl),15-(3,5-dimehoxyphenyl)porphyrin, 4 2,4,6-Triphenyl benzaldehyde was prepared by literature prodedure.[26] Purple crystal. Yield: 28.3%. *Anal.* Calcd for $C_{52}H_{38}N_4O_2$: C 83.18; H 5.10; N 7.46%; Found: C 83.32; H 5.13; N 7.47%. ^{1}H-NMR: δ −3.36 (s, 1H, N$\underline{H}$), −3.25 (s, 1H, N$\underline{H}$), 3.98 (s, 2H, C$\underline{H}_2$), 6.25—6.30 (m, 6H, $H_{16'}$, $H_{22'}$, $H_{15'}$, $H_{17'}$, $H_{21'}$, $H_{23'}$), 6.91 (t, 1H, $H_{4''}$), 6.92—6.95 (m, 4H, $H_{14'}$, $H_{18'}$, $H_{20'}$, $H_{24'}$), 7.38 (d, 2H, $H_{2''}$, $H_{6''}$), 7.51 (tt, 1H, $H_{10'}$), 7.63 (tt, 2H, $H_{9'}$, $H_{11'}$), 8.01—8.03 (dm, 2H, $H_{8'}$, $H_{12'}$), 8.07 (s, 2H, $H_{3'}$, $H_{5'}$), 9.07 (d, 2H, pyrrole βH), 9.09 (d, 2H, pyrrole βH), 9.18 (d, 2H, pyrrole βH), 9.29 (d, 2H, pyrrole βH), 10.11 (s, 2H, *meso*H). MS (ESI+): *m/z* obsd. 751.3058, calcd. 751.3073 $[M+H]^+$.

5-(2-Benzyloxy-1-naphthyl),10,15,20-tri(3,5-dimehoxyphenyl)porphyrin, 1′ Condensation of pyrrole (1 mmol), 2-benzyloxy-1-naphthaldehyde (0.25 mmol) and 3,5-dimethoxybenzaldehyde (0.75 mmol) started upon addition of $BF_3 \cdot OEt_2$ (0.33 mmol) at room temperature in dry chloroform (100 ml) under Ar atmosphere. After 1 h, a stoichiometric amount of DDQ dispersed in benzene was added quickly to convert the porphyrinogens to porphyrins. After evaporation of the solution to dryness, the residue was redissolved in a minimum of CH_2Cl_2 and chromatographed over a column of silica gel with CH_2Cl_2 as eluent. The eluate from the fifth red-fluorescent band was collected and again chromatographed over a column of silica gel with CH_2Cl_2 as eluent. The eluate from the first red-fluorescent band was evaporated and the residue was reprecipitated from dichloromethane–methanol, affording 25.4 mg (25.4% based on the statistical yield) of pure **2** (purple crystal). *Anal.* Calcd for $C_{61}H_{50}N_4O$: C 77.03, H 5.30, N 5.89%; Found: C 77.19, H 5.64, N 5.83%. ^{1}H-NMR: δ −2.62 (s, 1H, N$\underline{H}$), 3.94 (d, 12H, OC$\underline{H}_3$), 3.97 (d, 6H, OC$\underline{H}_3$), 5.00 (s, 2H, C$\underline{H}_2$), 6.55 (dm, 2H), 6.71 (tt, 2H), 6.84—6.87 (tt, 1H), 6.87 (t, 2H), 6.87—6.90 (dm, 1H), 6.91 (t, 1H), 6.947—7.02 (tm, 1H), 7.32—7.36 (tm, 1H), 7.38—7.44 (m, 6H), 7.70 (dd, 1H), 8.04 (dd, 1H), 8.25 (dd, 1H), 8.55 (d, 2H, pyrrole βH), 8.82 (d, 2H, pyrrole βH), 9.40 (s(t), 4H, pyrrole βH). MS (ESI+): *m/z* obsd. 951.3761, calcd. 951.3758 $[M+H]^+$.

References and Notes

1) Chou J. H., Nalwa H. S., Kosal M. E., Rakow N. A., Suslick K. S., "The Porphyrin Handbook," Vol. 6, Chap. 41, ed. by Kadish K. M., Smith K. M., Guilard R., Academic Press, San Diego, 2000, pp. 43—131.
2) Pandey R. K., Zheng G., "The Porphyrin Handbook," Vol. 6, Chap. 43, ed. by Kadish K. M., Smith K. M., Guilard R., Academic Press, San Diego, 2000, pp. 157—230.
3) Medforth C. J., "The Porphyrin Handbook," Vol. 5, Chap. 35, ed. by Kadish K. M., Smith K. M., Guilard R., Academic Press, San Diego, 2000, pp. 61—65.
4) Ghosh A., Almlöf J., *J. Phys. Chem.*, **99**, 1073—1075 (1995).
5) Maity D. K., Truong T. N., *J. Porphyrins Phthalocyanines*, **5**, 289—299 (2001).
6) Maity D. K., Mell R. L., Truong T. N., *J. Am. Chem. Soc.*, **122**, 897—906 (2000).
7) Reimers J. R., Lü T. X., Crossley M. J., Hush N. S., *J. Am. Chem. Soc.*, **117**, 2855—2861 (1995).
8) Smedarchina Z., Siebrand W., Wildman T. A., *Chem. Phys. Lett.*, **143**, 395—399 (1988).
9) Kenneth M. M., Jr., Reynolds C. H., *J. Chem. Soc., Chem. Commun.*, **1988**, 90—92 (1988).
10) Asakawa M., Toi H., Aoyama Y., Ogoshi H., *J. Org. Chem.*, **57**, 5796—5798 (1992).
11) Braun J., Limbach H. H., Williams P. G., Morimot H., Wemmer D. E., *J. Am. Chem. Soc.*, **118**, 7231—7232 (1996).
12) Kümmerl L., Kliesch H., Wöhrle D., Haarer D., *Chem. Phys. Lett.*, **227**, 337—342 (1994).
13) Braun J., Schlabach M., Wehrle B., Köcher M., Vogel E., Limbach H. H., *J. Am. Chem. Soc.*, **116**, 6593—6604 (1994).
14) Frydman L., Rossomando P. C., Sambrotta L., Frydman B., *J. Phys. Chem.*, **96**, 4753—4755 (1992).
15) Frydman L., Olivieri A. C., Diaz L. E., Valasinas A., Frydman B., *J. Am. Chem. Soc.*, **110**, 5651—5661 (1988).
16) Eaton S. S., Eaton G. R., *J. Am. Chem. Soc.*, **99**, 1601—1604 (1977).
17) Ortega H. G., Crusats J., Feliz M., Ribo J. M., *J. Org. Chem.*, **67**, 4170—4176 (2002).
18) Shaw S. J., Shanmugathasan S., Clarke O. J., Boyle R. W., Osborne A. G., Edwards C., *J. Porphyrins Phthalocyanines*, **5**, 575—581 (2001).
19) Crossley M. J., Field L. D., Harding M. M., Sternhell S., *J. Am. Chem. Soc.*, **109**, 2335—2341 (1987).
20) As can be seen later, non-averaged βH signals assigned to pyrrole rings with and without a proton on the pyrrole nitrogen were observed at slow exchange for **1′** (Fig. 5). It is very improbable that a chemical perturbation removing the 10- and 20-substituents from **1′** could give rise to incidental degeneracy of such two βH resonances. Furthermore, βH signal (H3 or 7) for **1** in CD_2Cl_2 showed obvious broadening with full width at half maximum *ca.* 43 Hz at 183 K. The preliminary simulation of this signal lead to a value of at least 70 Hz for the intrinsic splitting. The observation must be due to the two peaks arising from the pyrrole rings with and without a proton on the pyrrole nitrogen of **1**.
21) It was assumed that only exchange is responsible for the temperature-dependent line shapes. Actually, there is a possible temperature-dependent contribution from ^{14}N quadrupole-induced relaxation to the

line widths, and thus the assumption that only exchange is responsible for the line broadening would give the upper limits for the exchange rate constants.
22) Kano K., Fukuda K., Wakami H., Nishiyabu R., Pasternack R. F., *J. Am. Chem. Soc.*, **122**, 7494—7502 (2000).
23) Bond A. D., Feeder N., Redman J. E., Teat S. J., Sanders J. K. M., *Cryst. Growth Des.*, **2**, 27—39 (2002).
24) It could be partially due to tunneling effect that the rate of the k_2 process in compound **1** never retard at low temperature. But such effect would not be a dominant factor realizing the higher rate of the k_2 process compared to the k_1 process in the wide range of temperature.
25) Brückner C., Posakony J. J., Johnson C. K., Boyle R. W., James B. R., Dolphin D., *J. Porphyrins Phthalocyanines*, **2**, 455—465 (1998).
26) Suslick K. S., Fox M. M., *J. Am. Chem. Soc.*, **105**, 3507—3510 (1983).